

Contents lists available at [SciVerse ScienceDirect](http://SciVerse.Sciencedirect.com)

Computers & Geosciences

journal homepage: www.elsevier.com/locate/cageo

PhaseQuant: A tool for quantifying tomographic data sets of geological specimens

Premkumar Elangovan^{*,1}, Dominik C. Hezel², Lauren Howard, Robin Armstrong, Richard L. Abel³*Department of Mineralogy, Image and Analysis Centre, Natural History Museum, Cromwell Road, SW7 5BD, London, UK*

ARTICLE INFO

Article history:

Received 1 June 2011

Received in revised form

19 January 2012

Accepted 21 January 2012

Keywords:

Micro-CT
Tomography
Rock
Meteorite
ImageJ

ABSTRACT

Micro-CT is becoming an increasingly important tool for non-destructive analysis of rock specimens. One of the major challenges with micro-CT is to extract quantitative information as opposed to qualitative information from the datasets. In this paper, PhaseQuant – a new software tool for processing a micro-CT image stack – is introduced. PhaseQuant is an open source freeware distributed as an ImageJ plugin. PhaseQuant is a simple and easy-to-use software tool that comprises phase segmentation, phase measurement, validation and density calibration modules which together enable the user to follow a repeatable experimentation protocol for quantifying phases and components from a micro-CT image stack of rock specimens. The techniques used in the software tool are outlined in this paper along with some illustrative examples of application of the software to meteorites and rock cores. Detailed instructions on how to use the code are available on the Internet.⁴

© 2012 Elsevier Ltd. All rights reserved.

1. Introduction

Micro-CT is becoming an increasingly important tool for performing non-destructive analysis of rock specimens (Ebel and Rivers, 2007; Van Geet et al., 2001). Micro-CT scans of rocks are virtual models with gray values representing primarily the X-ray attenuation of different minerals or other features – such as pores – in the rock (Wellington and Vinegar, 1987). Since micro-CT has only recently been applied to geosciences and meteoritics, the technique has mostly been used qualitatively rather than quantitatively. Only lately progress has been made in the development of tools and methods for using micro-CT for quantitative analysis of rock specimens. Texture-based image segmentation methods (Friedrich, 2008b) and histogram thresholding methods (Long et al., 2009) have been applied for automatic segmentation of the phases from the image stack. Further, there have been significant improvements in acquisition of the particle size distribution and abundance (Friedrich et al., 2008a; Ebel et al., 2008), orientation (Ketcham, 2005b) and porosity measures (Long et al., 2009) from the micro-CT stack. The software BLOB3D (Ketcham, 2005a) is a popular tool that is currently being used

for isolating, visualizing and quantifying particles from an image stack. Nonetheless, quantifying CT data of rock specimens is still in its infancy.

The challenges in using micro-CT for rock studies are (a) artefacts such as beam hardening and rings caused by the polychromatic X-ray beams (Remeysen and Swennen, 2006) and electronic noise in the detector panel, respectively; (b) partial volume averaging due to limitations on voxel size; (c) overlap in CT numbers of phases with similar densities (Elangovan et al., 2010, Griffin et al., 2012). Further, each rock specimen is unique in texture and mineralogy (Thorpe and Brown, 1993) and this makes it difficult to have a specific method that gives consistent performance across a wide variety of specimens. There is the requirement for an open source tool that is expandable and easy to use and at the same time establishes a repeatable experimentation protocol for quantifying micro-CT image stacks.

PhaseQuant is an in house Java Plug-in that segments and quantifies mineralogical phases and/or components in rock specimens and performs measurements. PhaseQuant is built upon the Java Swing architecture and distributed as a zip file, which can be installed as a plugin in ImageJ. PhaseQuant software, user manual and latest information on the plug-in are available for download on the Internet (see footnote 4). ImageJ is an open source image analysis tool developed by the National Institutes of Health (NIH) and applied by many users worldwide (NIH; Abramoff et al., 2004). It is an active platform for exchanging imaging code by many researchers. The reason for choosing ImageJ to distribute

* Corresponding author. Tel.: +44 7712403034.

E-mail address: premkumar.elangovan@gmail.com (P. Elangovan).

¹ Now at: Department of Electronic Engineering, University of Surrey, Guildford, GU2 7XH, Surrey, UK.

² Now at: Department of Geology and Mineralogy University of Cologne, Zùlpicher Str. 49b, 50674 Köln, Germany.

³ Now at: Department of Surgery and Cancer, Faculty of Medicine, Imperial College, Charring Cross Hospital, London, W6 8RF, UK.

⁴ <http://www.cosmoprograms.com>.

the code is its popularity, open source structure and ease of use. ImageJ plug-ins are easily expandable in terms of functionality as they offer interoperability with other plug-ins. PhaseQuant, being an ImageJ plugin-in, offers similar advantages and this leads to a faster development as some of the modules were extended from existing ImageJ modules and plug-ins. PhaseQuant is written to look like a standalone application esthetically, but from a coding perspective it is similar to other plug-ins in functionality.

PhaseQuant was developed to accomplish the following (a) to establish tools to perform repeatable experiments on micro-CT data (b) make this an open standard for incorporation of previous and future techniques of phase quantifications (c) to have a simple and easy tool with intuitive graphical user interface (GUI) (d) to address shortcomings of ImageJ in handling large datasets and (e) to incorporate smart memory management options to increase the run-time memory.

The idea behind making PhaseQuant open source and easily expandable is to set a stage for other researchers to exchange their techniques. This will eventually result in a collection of tools that will serve as a standard protocol that could be applied across a wide variety of geological specimens.

2. The PhaseQuant software

The central element of the PhaseQuant program is its GUI, which consists of toolbars, buttons, panes and a drawing canvas (Fig. 1). PhaseQuant requires an open image or a stack for the plug-in to load. The basic elements of PhaseQuant are *Collective Histogram*, *Running Histogram* and *Update Histogram*. These elements control the content displayed in the canvas. The *Collective Histogram* utility displays a cumulative histogram of the stack in the canvas. The *Running Histogram* utility displays the histogram corresponding to the current slice in the canvas and updates them as the current slice in the stack is changed. ImageJ has an extensive collection of imaging plug-ins such as filters, calculators, morphology etc. All the ImageJ plug-ins can be used simultaneously on the image stack while PhaseQuant is

executing. The *Update Histogram* utility will enable the user to register the changes made to the image stack by external plug-ins to PhaseQuant without having to restart the plug-in.

Multithreading is used in PhaseQuant to stop the GUI from freezing while performing tasks. Each task starts a new thread and a progress bar is associated with the task. The progress bar continues to update the status throughout the lifecycle of the task. This will enable the user to perform multiple tasks simultaneously and keep track of them. The limit on the number of parallel threads that can be run depends on the number of processors available in the underlying hardware.

PhaseQuant contains four modules, (1) *Phase Extraction* implements supervised, i.e., requires prior information using training data, and unsupervised, i.e., automatic image segmentation methods; (2) *Phase Measurement* includes measurement options such as porosity, modal abundance and size distribution; (3) *Ground Truth Optimization* enables the user to input a ground truth image and perform comparison between the user's and software measurements and (4) *Density Calibration* allows the user to include density standards and calibrate the micro-CT image stack. In the following we outline how these modules operate. Detailed information how to operate the program is provided in the manual that is available for download on the Internet (see footnote 4).

2.1. Phase extraction module

PhaseQuant enables the user to segment micro-CT data of rock specimens into various components or phases, acquire measurements and subsequently validate them against ground truth data (Section 2.3). Phases or components with large density contrasts, e.g., silicate and sulfides /metal can be manually thresholded with good accuracy. In contrast, silicate minerals usually have large density overlaps and it is impossible to segment those using simple global thresholds. To solve this, PhaseQuant provides a set of automated statistical segmentation methods that are not based on simple thresholding (cf. Griffin et al., 2012). These methods also enable consistency in segmentation between users. The

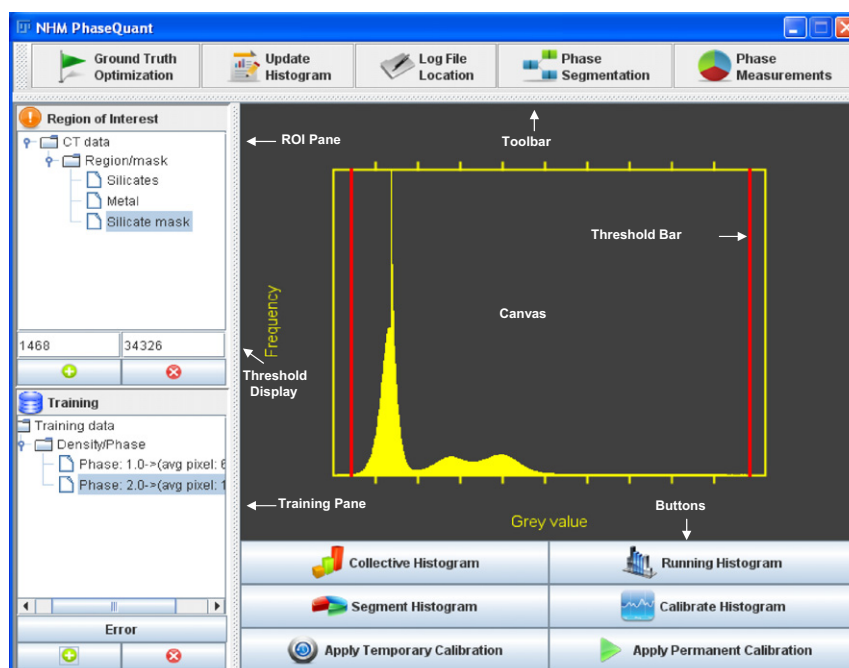


Fig. 1. Graphical user interface of PhaseQuant.

methods so far built in to PhaseQuant are: Kmeans clustering, Parzen windows, Bayesian decision and Windowing methods.

Segmentation methods used in PhaseQuant can be broadly classified into three types (a) non-parametric methods (Kmeans clustering & Parzen windows): these methods are based on some heuristic assumptions which if true for a specific dataset will result in good segmentation accuracy; (b) parametric methods (Bayesian decision) are based on explicit probabilistic models and requires training data for building the models and (c) hybrid methods (windowing methods) are a combination of non-parametric/parametric methods and image based morphological operations.

Intensity distribution or gray value distribution of a phase can be modeled as a Gaussian distribution of a specific mean and variance, similarly, overlapping intensity values of the phases can be modeled as a mixture of Gaussians. This is a fundamental assumption on which all the segmentation methods in PhaseQuant are built upon. The non-parametric methods, Kmeans clustering and Parzen windows are based on the heuristic assumption that the variances of the overlapping phases are equal. These methods perform well when the structure of the overlapping phases is proportional as shown in Fig. 2(a). The parametric method, Bayesian decision is suitable when the variances of the overlapping phases are disproportionate as shown in Fig. 2(b). The hybrid methods Windows-NN and Bayesian-NN are appropriate when the user wants to use either parametric or non-parametric method for basic classification, but classify the pixels close to the decision boundary (close to threshold) based on morphological image operation to emphasize the shape of the phases. A user can either make a subjective decision on the method by looking at the structure of the histogram or by trying different methods on one slice of the stack and then using the *Ground Truth Optimization* module explained in Section 2.3 to evaluate the best method for a given specimen.

Here we provide only brief explanations on the methods, for in-depth explanation readers are encouraged to refer to Duda et al. (2001) and Jain (2010). With Kmeans clustering, the process starts with a guess on the threshold and the dataset is partitioned into two classes and then cluster means are computed. A new threshold is computed from new cluster means and the process is repeated again. The cluster means are updated on every iteration and the process is continued until the cluster means converge, i.e., there is no or insignificant change in cluster means between iterations. In Parzen windows, the Gaussian kernels are constructed around the training samples and the decision is made based on the likelihood estimates for various classes. In Bayesian decision, a decision rule for segmentation is constructed from the probability distribution of the training dataset of different classes (Gaussian fit on training samples), which is then used for segmentation. In Windowing-NN (Nearest Neighborhood) which does not require training data, the Kmeans clustering is applied to divide the data set into three clusters rather than two and the pixels classified in the middle cluster is treated as uncertain data. The uncertain data are assigned to either of the clusters using nearest neighborhood method. The nearest neighborhood method is based on the principle that the cluster membership of a pixel is likely to be same as that of its surrounding members. In Bayesian-NN which requires training data, the initial segmentation is performed by the Bayesian decision and the pixel is classified uncertain where outcome of the decision function is too close to the decision boundary. The uncertain pixels are further processed and assigned to a class based on nearest neighborhood method. On application of a segmentation algorithm, PhaseQuant creates a mask containing discrete gray values representing the segmented phases. Fig. 3 shows a micro-CT slice of a meteorite (Allende, CV3) and the corresponding output mask after processing with Windowing-NN. We have more segmentation

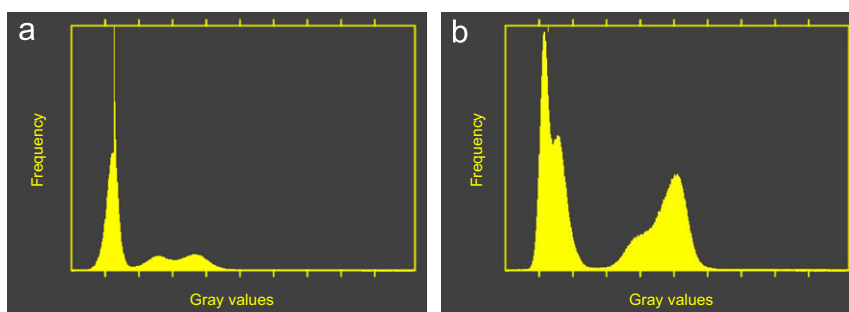


Fig. 2. (a) Symmetric histogram and (b) asymmetric histogram.

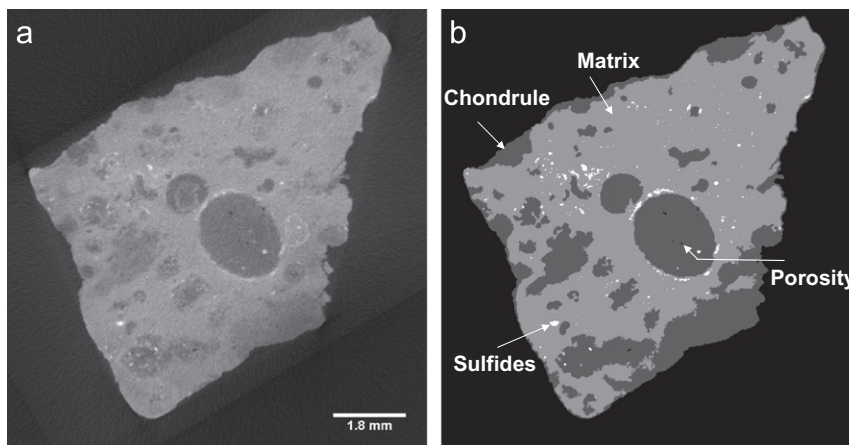


Fig. 3. (a) Allende CV3 meteorite and (b) mask generated after processing via PhaseQuant tool.

methods under development, which will be added to the software after testing and validation.

Other utilities in PhaseQuant comprise *Cluster Analysis* to perform object analysis on segmented phases, *3D Morphological Tool* to de-pixelate and emphasize object boundaries, *Combine Mask* to combine masks created by various methods and *Reduce Border* to reduce the size of the specimen by stripping away the outer layer. The *Cluster Analysis* utility under the *Phase Extraction* module will enable the user to analyze the connectivity characteristics of objects. Though the morphological tool in ImageJ and *Cluster Analysis* in PhaseQuant are based on the principle of opening or closing the image by a series of dilation and erosion operations, the major difference is that the former operates on the pixels and the later operates on the objects. *Cluster Analysis* offers the flexibility of specifying maximum and minimum bounds on the object size of each phase. Fig. 4 shows the result of cluster analysis on an Allende meteorite mask (segmentation performed by Kmeans clustering) in which the minimum cluster size of matrix and chondrule phases is set to 40 and 15 pixels, respectively and the clusters smaller than the specified size have been blended into the background. *Reduce Border* utility under *Phase Segmentation* module will enable the user to reduce the outer diameter of the specimen by a few pixels. This is necessary because a distinct layer of pixels with spurious gray values forms at the boundary between the air and the specimen due to partial volume averaging effect and has a quite significant impact on the performance of segmentation and subsequent measurements. Fig. 5 shows the mask (segmentation performed by Windowing-NN method) before and after reduction in the size of the specimen to remove the erroneous boundary.

2.2. Phase measurement module

After phase segmentation, PhaseQuant can perform measurements on the segmented dataset. The measurement options in PhaseQuant include *Modal Abundance*, *Object/Size Distribution*, *Porosity* and *Inter-phase Distribution*. *Modal Abundance* calculation in PhaseQuant does not rely on the *StackStatistics* or *ImageStatistics* classes, which are used by ImageJ to store the histogram data to overcome the storage limitation issue explained in Section 3. Instead, PhaseQuant directly operates on the image stack to collect measurements. This results in accurate voxel count of 3D modal abundances regardless of the size of the image stack.

The *Object/Size Distribution* (2D) utility counts the number of clusters in a 2D slice and generates size distribution data and an object mask identifying each cluster with a different gray value. Though this utility is similar to existing ParticleAnalyzer utility in

ImageJ, the limitation of ParticleAnalyzer is that it requires a binary mask as an input and with the PhaseQuant utility it is possible to process non-binary masks with multiple phases without having to separate them into a series of binary masks. The *Object/Size Distribution* (3D) utility in PhaseQuant just calls the existing Object Counter3D ImageJ plug-in (Bolte and Cordelières, 2006), but ObjectCounter3D suffers from similar disadvantages as ParticleAnalyzer as it can only process stacks with one phase. This issue is being addressed at the moment by extending 2D *Object/Size Distribution* in PhaseQuant to 3D and this utility will be available in the next release of PhaseQuant. Fig. 6 illustrates the output of 2D *Object/Size Distribution* utility in PhaseQuant.

The *Porosity* utility computes void space in the image stack. In order to do this, the bulk of the specimen must be thresholded out from the background and fed into the *Porosity* module. PhaseQuant uses *BinaryFiller* and *ImageCalculator* classes from ImageJ to compute the porosity. The stack image is first duplicated to two copies and then *BinaryFiller* is executed on one of the copies, which fills up all the void spaces. Subsequently *ImageCalculator* is used to subtract the copies from each other. The resulting image is a mask with non-zero intensity values corresponding to void locations in the image. Void spaces connected to the background are not classified as porosity since most of these void spaces are indications of a split in the specimen rather than a pore. Fig. 7 shows the output of porosity measurement acquired using PhaseQuant.

The *Inter-phase Distribution* utility is particularly useful when it is necessary to understand the distribution of a particular phase across different components of the sample. For example, in meteorites, this utility can be used to determine the opaque phase distribution and the modal abundances between matrix and chondrules, the two major components in chondrites. The *Inter-phase* utility requires two images as input, one image with two segmented phases and another image with just one phase. PhaseQuant iterates over pixel values in the second image and replaces them with a pixel value corresponding to the most likely enclosing phase from the first by investigating eight surrounding neighbors. Later, in order to ensure that each connected cluster in the second image is assigned a uniform gray value, *Cluster Analysis* is performed and all the pixels belonging to each cluster are replaced with the most repeated gray value within the cluster. Fig. 8 shows the *Inter-Phase Distribution* measurement performed on sulfides. After processing, the pixel values of the sulfide clusters are replaced with intensity values of the surrounding phases. This measurement is particularly useful for the estimation of accurate modal abundances of chondrules and matrix in meteorites as the metals/sulfides are added to the part of the phase in which they are enclosed.

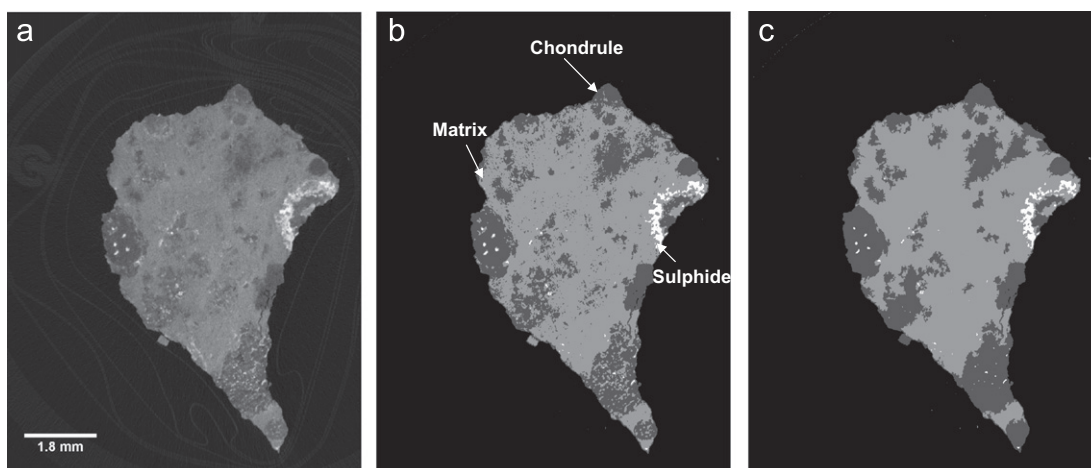


Fig. 4. (a) Allende CV3 meteorite (b) mask generated after segmentation (c) mask after performing cluster analysis.

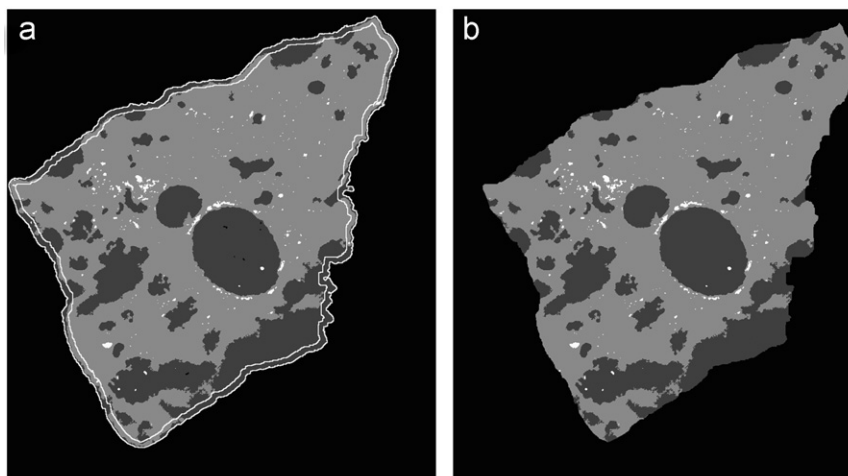


Fig. 5. (a) Allende CV3 meteorite mask after segmentation with erroneous outer border due to partial volume averaging (b) resulting mask after reducing the outer diameter by 10 pixels.

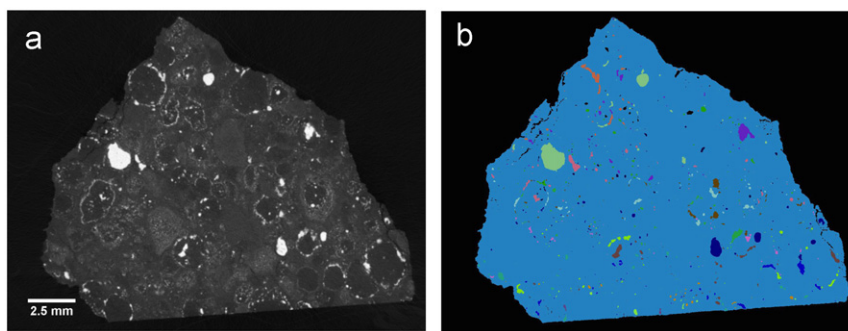


Fig. 6. Slices from Renazzo meteorite (a) before and (b) after object mask of metals generated by PhaseQuant.

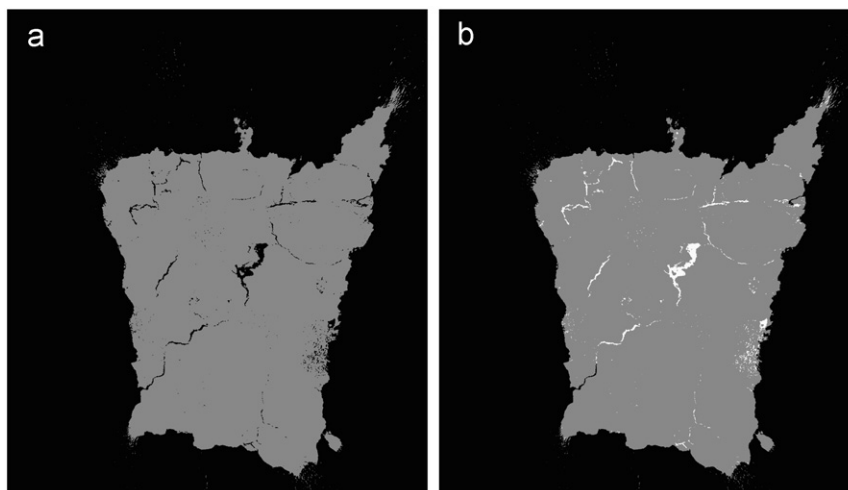


Fig. 7. Mask of (a) segmented bulk (b) after porosity measurement.

2.3. Ground truth optimization module

The automated segmentation methods, in most cases, cannot fully separate the different phases or components, as there is a certain error associated with these methods. PhaseQuant has a method built in that validates the segmented masks against ground truth (GT) data generated either from manual labeling of a CT slice or from phase maps acquired with a scanning electron microscope (SEM). The choice of the appropriate method for GT generation will depend on the specimen, as the SEM will

require the specimen to be serial sectioned and processed for analysis. Once ground truth information is available, PhaseQuant can be used to measure the segmentation accuracy and generate an error map to visualize the deviation. PhaseQuant performs a pixel-by-pixel comparison between the phases in GT and the corresponding phases in the mask and highlights the discrepancy in the error map. Further, PhaseQuant also quantifies the error in absolute percentage with respect to the slice dimensions and displays them in a popup window. PhaseQuant requires GT data to be of the same resolution as the mask and must contain

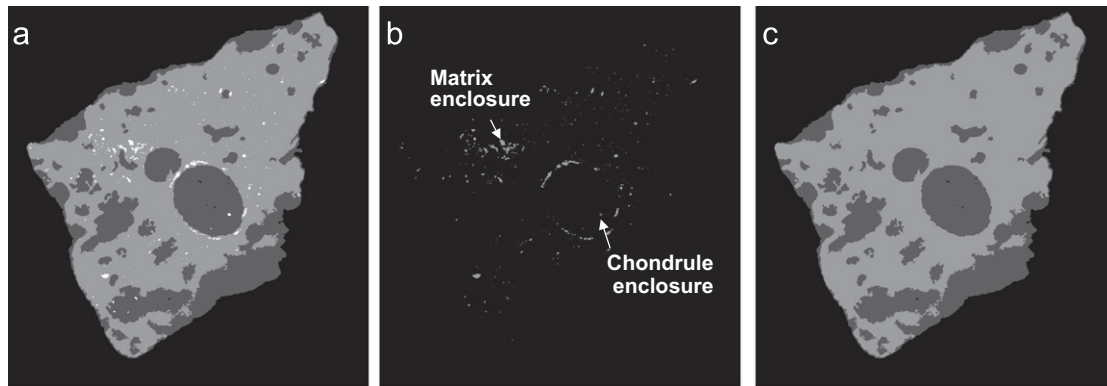


Fig. 8. (a) Mask after segmentation (b) mask after inter-phase distribution measurement (c) mask after replacing opaques with inter-phase distribution data.

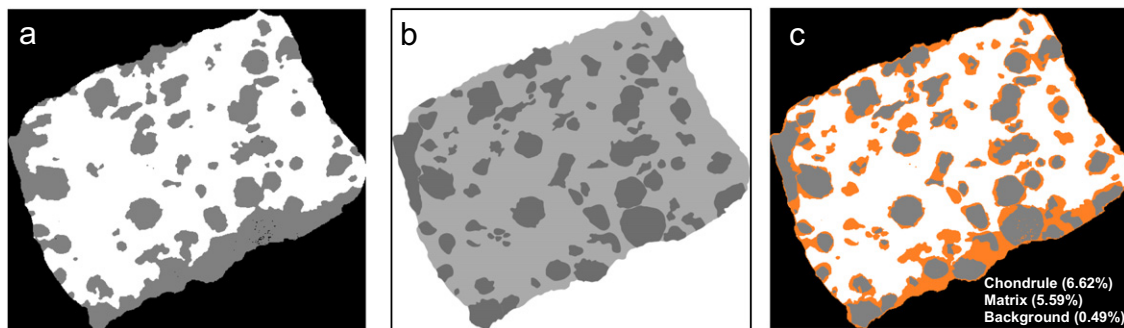


Fig. 9. (Color online) (a) Segmented mask obtained from PhaseQuant (b) Ground truth image of Allende slice generated by manual labeling (c) Error mask after ground truth optimization highlighting the discrepancy between segmented mask and ground truth image along with error percentage.

discrete values representing different phases. In reality, a GT acquired from SEM may be of higher resolution and must be scaled down before loading into PhaseQuant. Fig. 9 illustrates the output of the *Ground Truth Optimization* module and the error map highlights the discrepancy between GT image and PhaseQuant mask image in orange color.

2.4. Density calibration module

The “virtual” specimens resulting from micro-CT scans are made up of voxels, the 3D equivalent of pixels, each assigned a gray value based on X-ray absorption. The gray values are influenced by various factors other than density such as beam hardening, surrounding components, atomic number and thickness and as a result, the relative contrast between the phases does not accurately represent the relative densities. Further, there is a considerable variation across the image stacks in terms of dynamic range and contrast that are acquired from scanning the same specimen multiple times under similar conditions due to changes in X-ray flux. This results in inconsistencies in thresholding across different specimens with similar material phases.

Density calibration is important for standardising scans so that (a) comparable segmentation and measurement protocols can be applied and (b) these steps can be automated and batched more easily. PhaseQuant has a utility with which the user can assign a certain gray value to a corresponding density. This allows the generation of a calibration curve for density vs. gray values, when density standards are scanned together with the sample. After calibration, the image stack generated by performing multiple scans on the same sample would have consistent gray values, and also it is possible to apply the same threshold values for separating out the phases, which is not possible before calibration. Detailed working of the *Density Calibration* module and

experimental results of application of calibration to a rock core are presented in Howard et al. (2011) and Dominy et al. (2011).

3. Software challenges

One of the shortcomings of ImageJ is its inability to handle large datasets. If an extremely large dataset is processed in ImageJ, it results in histograms with negative bin counts. This is because ImageJ uses Integer data type to store bin counts. The maximum value that could be stored in an Integer data type is $2^{31} - 1$, when ImageJ tries to store a value bigger than this capacity; it results in an error that consequently results in negative bin counts. This problem has been effectively addressed in PhaseQuant by using the Long variable to store the values while computing modal abundance. Long variable has a bigger capacity than Integer and maximum value that could be stored is $2^{63} - 1$.

The size of a single micro-CT stack can be over 40 GB and in order to process the stack it must be loaded into RAM. Furthermore, every time a new mask is created as a result of segmentation additional space is allocated in the RAM in order to accommodate the new mask. It is crucial that the memory space is continuously monitored within the program to stop ImageJ from running out of storage space. Java runs garbage collector to free memory space: A module that is used by Java to remove unused space as the available memory goes below a certain level. It is hard to predict how and when Java runs its garbage collector and in some instances it does not happen until the program totally runs out of memory. On deletion of a mask, PhaseQuant tries to force the garbage collector to free up memory space rather than to wait for the Java Virtual Machine (JVM) to run the collector, though this measure may not be successful on all occasions. This process is intended to ensure that the memory is available instantly in runtime as is crucial when operating on a large dataset.

4. Conclusions

With micro-CT being applied widely to geosciences and meteoritics, it becomes important to develop powerful tools to extract quantitative information from the tomographic datasets. The PhaseQuant program provides a structural framework for quantifying micro-CT datasets. The software was constructed to allow for updates and incorporation of additional tools and can be continuously incremented as new imaging methods are tried out on rock specimens. Future work should involve integrating other promising phase segmentation methods in existence. The core strength of PhaseQuant is its usability and graphical user interface. Any user familiar with ImageJ will have no difficulty using PhaseQuant. PhaseQuant is highly generic freeware, but as such can be made available in the public domain for reuse or expansion and customized for specific end-user requirements.

Acknowledgments

This project was funded by the Natural History Museum Strategic Initiative Fund (2010–2011). We also thank the Snowdon Group for providing rock core samples. We thank Jon M. Friedrich and Richard Ketcham for their thoughtful reviews that significantly improved this work.

References

- Abramoff, M.D., Magelhaes, P.J., Ram, S.J., 2004. Image processing with ImageJ. *Biophotonics International* 11, 36–42.
- Bolte, S., Cordelières, F.P., 2006. A guided tour into subcellular colocalization analysis in light microscopy. *Journal of Microscopy* 224, 213–232.
- Dominy, S.C., Platten, I.M., Howard, L.E., Elangovan, P., Armstrong, R., Minnitt, R.C.A., Hezel, D.C., Abel, R.L., 2011. Characterisation of gold ores by X-ray computed tomography – Part 2: Applications to the determination of gold particle size and distribution. In Proceedings of the First AusIMM International Geometallurgy Conference, Brisbane, Australia, 5–7 Sep 2011.
- Duda, R.O., Hart, P.E., Stork, D.G., 2001. *Pattern Classification*. Wiley, Toronto. Chapters 2–4.
- Ebel, D.S., Rivers, M.L., 2007. Meteorite 3D synchrotron microtomography: methods and applications. *Meteoritics & Planetary Science* 42, 1627–1646.
- Ebel, D.S., Weisberg, M.K., Hertz, J., Campbell, A.J., 2008. Shape, metal abundance, chemistry, and origin of chondrules in the Renazzo (CR) chondrites. *Meteoritics & Planetary Science* 43, 1725–1740.
- Elangovan, P., Abel, R., Hezel, D.C., Armstrong, R., 2010. Automatic phase segmentation of chondrule and matrix from micro-CT meteorite slices. Abstract presented at Paneth Kolloquium, Nördlingen, Germany, 3.
- Friedrich, J.M., Macke, R.J., Wignarajah, D.P., Rivers, M.L., Britt, D.T., Ebel, D.S., 2008a. Pore size distribution in an uncompacted equilibrated ordinary chondrite. *Planetary and Space Science* 56, 895–900.
- Friedrich, J.M., 2008b. Quantitative methods for three-dimensional comparison and petrographic description of chondrites. *Computers and Geosciences* 34, 1926–1935.
- Griffin, L.D., Elangovan, P., Mundell, A., Hezel, D.C., 2012. Improved segmentation of chondrules from micro-CT images of meteorites using local histograms. *Computers & Geosciences* 39, 129–134.
- Howard, L., Elangovan, P., Dominy, S., Armstrong, R., Hezel, D.M., Platten, I., Abel, R.L., 2011. Characterisation of gold ores by X-ray computed tomography Part 1: Software for calibration and quantification of mineralogical phases. In: Proceedings of the First AusIMM International Geometallurgy Conference, Brisbane, Australia, 5–7 Sep 2011.
- Jain, A.K., 2010. Data clustering: 50 years beyond Kmeans. *Pattern Recognition Letters* 31, 651–666.
- Ketcham, R.A., 2005a. Computational methods for quantitative analysis of three-dimensional features in geological specimens. *Geosphere* 1, 32–41.
- Ketcham, R.A., 2005b. Three-dimensional grain fabric measurements using high-resolution X-ray computed tomography. *Journal of Structural Geology* 27, 1217–1228.
- Long, H., Swennen, R., Foubert, A., Dierick, M., Jacobs, P., 2009. 3D quantification of mineral components and porosity distribution in westphalian C Sandstone by microfocus X-ray computed tomography. *Sedimentary Geology* 220, 116–125.
- NIH. ImageJ: Image Processing and Analysis in Java. [Online]. National Institute of Health. <<http://rsbweb.nih.gov/ij/>>.
- Remeysen, K., Swennen, R., 2006. Beam hardening artifact reduction in microfocus computed tomography for improved quantitative coal characterization. *International Journal of Coal Geology* 67, 101–111.
- Thorpe, R., Brown, G., 1993. *The field description of igneous rocks*. Geological Society of London Handbook. Wiley, Chichester.
- Van Geet, M., Swennen, R., Wevers, M., 2001. Towards 3D petrography: application of microfocus computer tomography in geological science. *Computers & Geosciences* 27, 1091–1099.
- Wellington, S.L., Vinegar, H.J., 1987. X-ray computerized tomography. *Journal of Petroleum Technology* 39, 885–898.